

A K-band SiGe Super-Regenerative Amplifier for FMCW Radar Active Reflector Applications

Manu V. Thayyil, Songhui Li, Niko Joram and Frank Ellinger, *Senior Member, IEEE*

Abstract—A K-band integrated super-regenerative amplifier (SRA) in a 130 nm SiGe BiCMOS technology is designed and characterized. The circuit is based on a novel stacked transistor differential cross-coupled oscillator topology, with a controllable tail current for quenching the oscillations. The fabricated integrated circuit (IC) occupies an area of 0.63 mm², and operates at the free-running center frequency of 25.3 GHz. Characterization results show circuit operation from a minimum input power level required for a phase coherent output as -110 dBm, and the input power level corresponding to the linear to logarithmic mode transition of -85 dBm, the lowest reported for K-band integrated logarithmic mode SRAs to date to the knowledge of the authors. The measured output power is 7.8 dBm into a 100 Ω differential load. The power consumption of the circuit is 110 mW with no quench signal applied, and 38 mW with 30 % duty cycle quenching. The quench waveform designed for the reported measurement result is also discussed.

Index Terms—Super-regenerative amplifiers, K-band, FMCW radar, SiGe, BiCMOS, cross-coupled oscillators.

I. INTRODUCTION

The super-regeneration principle [1] explains the possibility of input signal amplification by an oscillator when oscillations are periodically quenched by a quench signal. Since the core of the amplification process is a single port oscillator, the super-regenerative amplifier (SRA) when used in communication receiver applications acts also as a transmitter, causing significant interference [2]. Nevertheless, key features of the circuit including low complexity, high gain and low power consumption gives it other interesting prospects. Of particular interest is the use of super-regenerative circuits as active reflectors for frequency modulated continuous wave (FMCW) radar and pulse radar based positioning and localization systems as introduced in [3]. Radar active reflector applications take advantage of both radiated power and input signal sensitivity.

Several implementations of integrated logarithmic mode SRAs targeting radar reflector applications are found in literature [3], [4], [5]. These circuits exhibit a trade off between the maximum output power delivered to the load and the minimum input power that can be detected. This work introduces a novel differential stacked transistor cross-coupled oscillator topology to improve the output power and the quench waveform required to simultaneously improve minimum input power level for phase coherent output.

Manuscript received September 7, 2017; revised January 31, 2018 and April 13, 2018; accepted May 11, 2018. This work has received funding from the European Union's Horizon 2020 research and innovation programme under grant agreement No 636286 (Lynceus2Market).

The authors are with the Chair for Circuit Design and Network Theory, Technische Universität Dresden, 01069 Dresden, Germany (email: manu.thayyil@tu-dresden.de)

The design of the stacked transistor cross-coupled SRA is discussed in Section II-A. The investigation of the influence of the quenching waveform on circuit performance follows in Section II-B. Characterization methodology and results are reported in Section III. Section IV summarizes the work by comparing the results with state-of-the-art FMCW active reflector implementations.

II. DESIGN

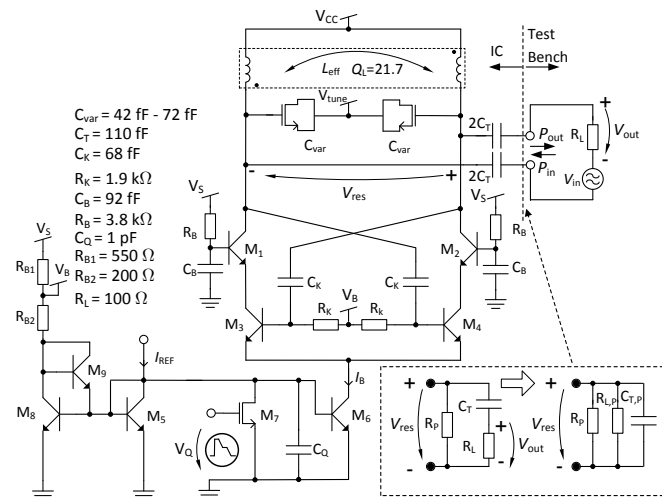


Fig. 1: Circuit schematic of the super-regenerative amplifier.

A. Stacked transistor cross-coupled quenched oscillator

The core of the SRA shown in Fig. 1 is a cross-coupled pair formed by transistors $M_{3,4}$, along with series stacked transistors $M_{1,2}$ with base termination C_B and R_B . The resonator is formed by an on-chip symmetrical center tapped spiral inductor L_{eff} , and effective capacitance C_{eff} . C_{eff} is the equivalent of the varactor capacitance C_{var} , the base-collector capacitor of transistors $M_{1,2}$ in series with C_B , and the feedback capacitance C_K in series with the input capacitance of transistors $M_{3,4}$, and layout parasitics. Oscillation frequency $\omega_{\text{osc}} = \frac{1}{\sqrt{L_{\text{eff}}C_{\text{eff}}}}$ is tuned by varying the bias of MOS varactors V_{tune} to change the capacitance C_{var} , resulting in an oscillation frequency range from 24.4 GHz to 25.8 GHz. The inductor $L_{\text{eff}} = 130$ pH is optimized for an unloaded quality factor $Q_L \approx 21.7$, corresponding to an equivalent parallel resistance $R_P = Q_L \omega_{\text{osc}} L_{\text{eff}} \approx 448 \Omega$ at $f_{\text{osc}} = 25$ GHz. The output power is delivered to the load resistance $R_L = 100 \Omega$ through

coupling capacitors $2C_T = 220$ fF. The network formed by R_L and C_T , can be transformed to equivalent parallel network across the resonator, with $R_{L,P} = R_L \cdot (1 + Q_{R_L,C_T}^2) = 133 \Omega$ and $C_{T,P} = \frac{C_T \cdot Q_{R_L,C_T}^2}{(1 + Q_{R_L,C_T}^2)} \approx 27$ fF. Q_{R_L,C_T} is the quality factor of the series load transfer network defined as $Q_{R_L,C_T} = \frac{1}{\omega_{osc} R_L C_T} \approx 0.58$ at $f_{osc} = 25$ GHz. The parallel combination of calculated $R_{L,P}$, and R_P gives the effective parallel resistance across the resonator R_{eff} of 102Ω , and resonator quality factor $Q_{res} = \frac{R_{eff}}{\omega_{osc} L_{eff}} \approx 5$. The series equivalent network shown in Fig. 1 also forms a potential divider, with $\frac{|V_{out}|}{|V_{res}|} = \left| \frac{R_L}{R_L - jX_{C_T}} \right|$, giving $V_{out,pk-pk} \approx V_{res,pk-pk} \cdot 0.865$. Where, $V_{out,pk-pk}$ and $V_{res,pk-pk}$ are the differential peak to peak voltage swings at the load resistor and resonator respectively, and $X_{C_T} = \frac{1}{\omega_{osc} C_T}$. From an output power requirement of $P_{out,dBm} = 8$ dBm, the peak to peak differential voltage swing can then be calculated as $V_{out,pk-pk} = 2.24$ V. This corresponds to a single ended peak to peak voltage swing at collector of transistors $M_{1,2}$, $V_{C,M_{1,2},pk-pk} = \frac{V_{res,pk-pk}}{2} = 1.3$ V. The voltage swing has to be made higher as $V_{C,M_{1,2},pk-pk} = 1.6$ V to account for parasitics from transistors and layout. A bias current $I_B \approx 40$ mA is used to obtain this voltage swing. The heterojunction bipolar transistors (HBT) used for this design have the maximum available voltage swing of 1.05 V, due to the emitter to collector breakdown voltage $BV_{CEO} = 1.5$ V. To operate within the SOA, two stacked transistors, M_1 and M_2 are used. The effective breakdown voltage becomes 3 V, and the maximum available voltage swing at the collector of $M_{1,2}$ is now 2.1 V. The optimum values are calculated as $R_B = -\frac{R_{in,opt}^2 + X_{in,opt}^2}{R_{in,opt}} = 3.8$ k Ω and $C_B = \frac{1}{\omega_{osc}} \cdot \frac{X_{in,opt}}{R_{in,opt}^2 + X_{in,opt}^2} = 92$ fF from [6]. Where, $R_{in,opt}$ and $X_{in,opt}$ are the real and imaginary parts respectively of the input impedance of the stacked transistors obtained from simulations following a similar methodology as [6]. The feedback capacitor $C_K = 68$ fF is optimized to meet the startup requirements across process, voltage and temperature corners. Bias voltages V_B is generated using the biasing network shown in Fig. 1. In addition to making the circuit less sensitive to variations in process voltage and temperature, the biasing circuit also make sure that the emitter base breakdown voltage $BV_{EBO} = 1.2$ V on M_3 and M_4 are not exceeded when the oscillations are quenched, with the help of M_9 .

B. Quench Waveform Design

For using the SRA as an FMCW radar active reflector, characteristics of the step controlled logarithmic mode, corresponding to the quench signal $V_{q,w1}$ shown in Fig. 2(a) are preferred [4]. But, a linear, slope control mode is better for sensitivity [1]. The impact of slope on sensitivity can be visualized using the normalized Gaussian sensitivity window function $\mu(t)$ defined in Eq. (1) from [2] :

$$\mu(t) = e^{-\frac{1}{2} \frac{(t-t_0)^2}{\sigma^2}} \quad (1)$$

where t_0 is the time at which the resonator losses are equal to the time varying negative resistance, and $\sigma = \frac{1}{\sqrt{\omega_{osc} K_{w1}}}$. Here K_{w1} is the magnitude of the slope of the quench waveform

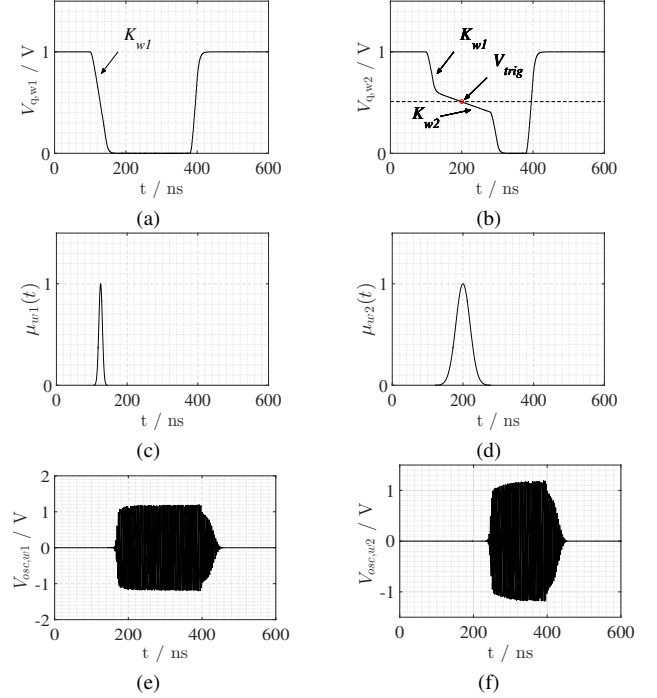


Fig. 2: The quench signal $V_{q,w1}$ is shown in (a), with corresponding normalized sensitivity curve $\mu_{w1}(t)$ in (c) and output oscillations $V_{osc,w1}$ in (e). The quench signal $V_{q,w2}$ is shown in (b), with corresponding normalized sensitivity curve $\mu_{w2}(t)$ in (d) and output oscillations $V_{osc,w2}$ in (f).

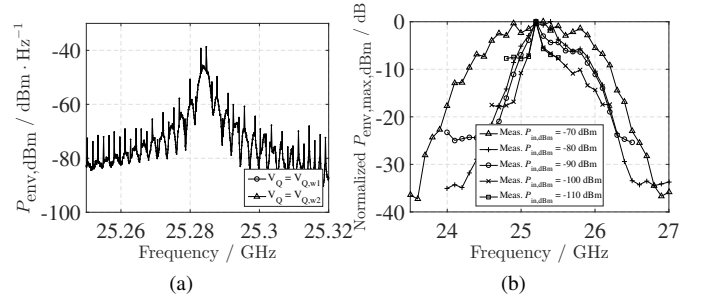


Fig. 3: (a) Plot of measured power spectral density with $P_{in,dBm} = -110$ dBm at $f_{osc} = 25.3$ GHz. (b) Normalized frequency response for different input power levels.

$V_{q,w1}$ near t_0 , and is defined as $V_{q,w1} = -K_{w1}t$. From [2], it is seen that an increase in σ and decrease in quench signal slope K_{w1} improves the input sensitivity. Simulation in Eq. (1) and measurement results in Section III show that this result can be exploited to improve the minimum input power level $P_{min,dBm}$ required for phase coherent output, at the same time maintaining a high quench rate. The quench waveform characteristics of the step and slope controlled modes are combined to create a dual slope quenching signal $V_{q,w2}$ shown in Fig. 2(b). At the beginning and end of the quench cycle, the designed two slope quench waveform $V_{q,w2} = -K_{w1} \cdot t$ is similar to the waveform $V_{q,w1}$. Then, near a trigger voltage V_{trig} , $V_{q,w2} = -K_{w2} \cdot t$, with $K_{w2} = 0.04 \cdot K_{w1}$ as shown in Fig. 2(b). This makes the sensitivity window $\mu(t)$ in Fig. 2(d)

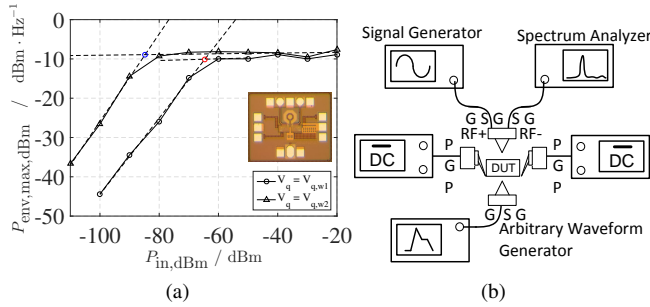


Fig. 4: (a) Plot of $P_{out,dBm}$ against $P_{in,dBm}$ for quench signals $V_{q,w1}$ and $V_{q,w2}$, with photograph of the IC measuring $875 \mu\text{m} \times 725 \mu\text{m}$ in inset. (b) Measurement setup illustration.

broader than $\mu(t)$ in Fig. 2(c), improving sensitivity [2], along with output power.

TABLE I: Comparison with State-of-The-Art FMCW Radar Active Reflectors

Ref.	f_{osc} [GHz]	$P_{min,dBm}$ [dBm]	$P_{i,N,dBm}$ [dBm]	$P_{out,dBm}$ [dBm]	BW [GHz]	P_{dc} [mW]	Tech.
[4]	34.5	-80	-67	5.6	0.5	122	250 nm BiCMOS
[7]	77	-66.4 ^a	NA	-14	5	18	45 nm SOI CMOS
[8]	24.125	-69 ^a	NA	5	0.24	42	130 nm CMOS
[9]	7-12	NA	NA	20-25	5	75	HEMT
This	25.3	-110	-85	7.8	0.25	110	130 nm BiCMOS

^aSensitivity calculated for 3 dB signal to noise ratio

III. CHARACTERIZATION

The designed integrated circuit shown in Fig. 4(a) inset is fabricated in a 130 nm Silicon-Germanium (SiGe) BiCMOS technology from IHP, and characterized by micro probing. Since time domain measurements of regenerative sampling is not practical at the frequencies of interest, frequency domain characterization is done as described in [4]. Parameters including f_{osc} , $P_{out,dBm}$, $P_{min,dBm}$ and bandwidth are characterized using the test setup consisting of a Rohde & Schwarz 67 GHz spectrum analyzer, Keysight 8257D RF power source, and an arbitrary waveform generator for quench generation as shown in Fig. 4(b). At first for each IC, the SRA is powered ON with quench signal $V_q = 0$ V to measure free-running oscillation frequency $f_{osc} = 25.3$ GHz, and the DC power consumption is measured as $P_{DC} = 110$ mW. Then, V_q is manually decreased from $V_q = 1$ V corresponding to no oscillations, until $V_q = V_{trig} = 670$ mV, where V_{trig} is the voltage at which oscillations just begin to start. Now, using an arbitrary waveform generator, the quench signal $V_{q,w2}$ is created and sourced, with input signal present. The corresponding *sinc* spectrum envelope, $P_{env,dBm}$ with Dirac delta spectral peaks separated by the quench frequency [4], indicating phase coherence as shown in Fig. 3(a) is then measured. A plot of the maximum of this spectral envelope $P_{env,max,dBm}$, when $P_{in,dBm}$ is varied is shown in Fig. 4(a). $V_{q,w2}$ is designed to have an ON time of 180 ns and a period of 600 ns, resulting in an average power consumption of 38 mW. The maximum quench signal frequency that can be used is 4.5 MHz. From Fig. 4(a), it is seen that with $V_{q,w1}$, $P_{min,dBm} = -100$ dBm

and for $V_{q,w2}$, $P_{min,dBm} = -110$ dBm. The slope of the curve at low input power level $P_{in,dBm}$ gives the linear mode super-regenerative gain of 66 dB with $V_{q,w1}$ and 85 dB with $V_{q,w2}$. As the circuit enters the logarithmic mode, gain compression occurs for $P_{in,dBm} > P_{i,N,dBm}$. For FMCW radar reflector, it is preferable to use the circuit for input power in the logarithmic region [5], and the parameter, $P_{i,N,dBm}$ denotes the input power level corresponding to the linear to logarithmic mode transition [4]. From the measurement data, $P_{i,N,dBm}$ is calculated as the intersection of the two extrapolated lines in Fig. 4(a). For $V_{q,w1}$, $P_{i,N,dBm} = -65$ dBm, and with $V_{q,w2}$, $P_{i,N,dBm} = -85$ dBm, clearly showing the advantage of $V_{q,w2}$. Bandwidth of the circuit is also an important parameter for FMCW radar applications as the localization resolution is directly proportional to bandwidth. The normalized frequency response when input frequency is swept over a range of values around f_{osc} is shown in Fig. 3(b), indicating a bandwidth increase with increased input signal power. A bandwidth of at least 500 MHz is available for $P_{in,dBm}$ greater than -90 dBm as seen in Fig. 3(b).

IV. CONCLUSION

The design of a K-band integrated SRA using a stacked transistor cross-coupled topology in a 130 nm BiCMOS technology, to be used as the core of an FMCW radar active reflector for localization systems is presented. Frequency domain characterization results of key parameters are compared with state-of-the-art designs in Table I showing that the designed circuit and quenching methodology clearly shows an improvement in the minimum input power level from which phase coherence is observed, $P_{min,dBm}$ of -110 dBm and the linear to logarithmic mode transition power $P_{i,N,dBm}$ of -85 dBm, combined with a high output power level of $P_{out,dBm}$ of 7.8 dBm.

REFERENCES

- [1] J. Whitehead, *Super-regenerative receivers*, ser. Modern radio technique. Cambridge University Press, 1950.
- [2] J. L. Bohorquez, S. Member, A. P. Chandrakasan, and J. L. Dawson, "Frequency-Domain Analysis of Super-Regenerative Amplifiers," *IEEE Trans. Microw. Theory Tech.*, vol. 57, no. 12, pp. 2882–2894, 2009.
- [3] M. Vossiek and P. Gulden, "The Switched Injection-Locked Oscillator: A Novel Versatile Concept for Wireless Transponder and Localization Systems," *IEEE Trans. Microw. Theory Tech.*, vol. 56, no. 4, pp. 859–866, 2008.
- [4] A. Strobel, C. Carlowitz, R. Wolf, F. Ellinger, and M. Vossiek, "A Millimeter-Wave Low-Power Active Backscatter Tag for FMCW Radar Systems," *IEEE Trans. Microw. Theory Tech.*, vol. 61, no. 5, pp. 1964–1972, 2013.
- [5] M. Schulz, N. Joram, C. Tzschoppe, and F. Ellinger, "Design of a Switched Injection-Locked Oscillator as an Active Backscatter Transponder for a 2.45 GHz FMCW Radar System," *Ger. Microw. Conf.*, pp. 267–270, 2016.
- [6] D. Fritsche, R. Wolf, and F. Ellinger, "Analysis and Design of a Stacked Power Amplifier With Very High Bandwidth," *IEEE Trans. Microw. Theory Tech.*, vol. 60, no. 10, pp. 3223–3231, 2012.
- [7] M. S. Dadash, J. Hasch, and S. P. Voinigescu, "A 77-GHz Active Millimeter-Wave Reflector for FMCW Radar," *Radio Freq. Integr. Circuits Symp.*, pp. 312–315, 2017.
- [8] A. Hamidian, R. Ebel, D. Shmakov, M. Vossiek, T. Zhang, V. Subramanian, and G. Boeck, "24 GHz CMOS Transceiver with Novel T/R Switching Concept for Indoor Localization," *Radio Freq. Integr. Circuits Symp.*, pp. 293–296, 2013.
- [9] J. Lorenzo, A. Lazaro, R. Villarino, D. Girbau, and S. Member, "Active Backscatter Transponder for FMCW Radar Applications," *IEEE Antennas Wirel. Propag. Lett.*, vol. 14, pp. 1610–1613, 2015.